Phys. Status Solidi A **209**, No. 5, 875–879 (2012) / **DOI** 10.1002/pssa.201100787

physica status solidi pss a
www.pss-a.com
applications and materials science

Biaxially textured copper–iron alloys for coated conductors

Bernhard Gallistl[1], Raimund Kirchschlager[2], and Achim Walter Hassel[*,1]

[1] Institute for Chemical Technology of Inorganic Materials, Johannes Kepler University, Altenberger Str. 69, 4040 Linz, Austria
[2] Institute for Semiconductor and Solid State Physics, Johannes Kepler University, Altenberger Str. 69, 4040 Linz, Austria

Received 8 November 2011, revised 30 March 2012, accepted 2 April 2012
Published online 19 April 2012

Keywords coated conductors, cube texture, magnetisation, RABiTS, tensile strength

[*] Corresponding author: e-mail achimwalter.hassel@jku.at, Phone: +43-732-24688700, Fax: +43-732-24688905

Two copper based biaxially textured alloys containing 0.37 and 0.91 wt.%-Fe have been investigated for the use as substrate material for coated conductors. Average full width at half maximum (FWHM) values of 7.3° (CuFe0.37) and 6.8° (CuFe0.91) for in-plane alignment and 7.2° (CuFe0.37, CuFe0.91) for out-of-plane are achieved. Ultimate tensile strength for the two alloys is found to be much higher compared to the values for Cu and CuFe2.35. Hysteresis losses are dramatically reduced compared to other available substrate materials. Magnetisation data for both alloys obtained at 5 K show an anticipated saturation magnetisation (M_s) $<0.35\ \mu Wb\ m\ kg^{-1}$, which is less than 1% of pure Ni.

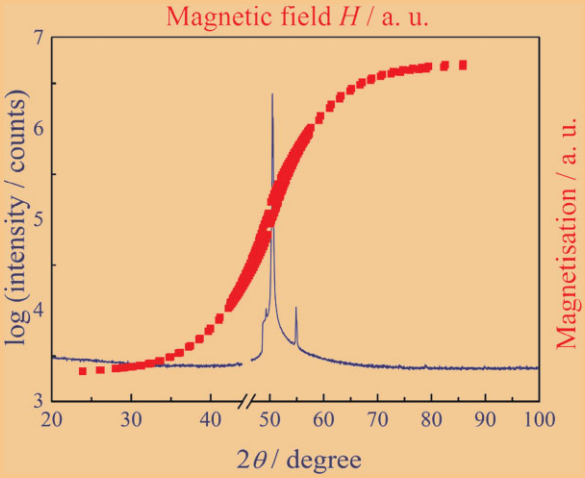

1 Introduction The design of suitable substrates for superconducting devices is still a challenging task. When selecting a metal or alloy as substrate material for coated conductors lots of different criteria such as lattice match with different buffer layers, oxidation resistance, texturability, tensile strength, magnetisation and so forth have to be considered. Nickel being the metal of choice in the early years of the rolling assisted biaxially textured substrates (RABiTS) process [1] soon turned out to suffer some major drawbacks. One major setback is the ferromagnetism of pure nickel which leads in AC applications to unwanted hysteresis and therefore to energy losses in the superconducting wire. Hence different alloys like Ni–Cr [2], Ni–W [3, 4] and Ni–Cr–W [5] are used to improve the magnetic properties of nickel.

Only in recent years copper and its alloys came into the focus of scientific discussion. The most prominent advantages of Cu are the absence of ferromagnetism, a sharp biaxial texture, large thermal and electrical conductivity and the low price compared to Ni and Ni-alloys (less than half). However copper suffers some disadvantages as well, like poor oxidation resistance and low tensile strength. Hence extensive research has been done to improve the oxidation resistance of Cu. This can be realised for instance using metal coatings [6], ceramic layers [7] or surface alloying [4]. To overcome the problem with low tensile strength Cu is alloyed, for example, with Ni [8] or Fe [9].

In contrast to the work done by Varanasi et al. who characterised similar alloys (2.35 wt.%-Fe) this report introduces two copper–iron alloys with low iron content (0.37 and 0.91 wt.%-Fe) and improved magnetic and mechanical properties.

2 Experimental details

2.1 Bulk samples The alloys (electrolytic tough pitch copper, Cu-ETP) and Fe powder (extra pure, Merck) were

molten in reducing hydrogen atmosphere (6.5% H_2, 93.5% Ar v/v) using an induction furnace (Linn High Term, Lifumat 10) and cast into ingots ($20 \times 20 \times 100\,mm^3$) using a stainless steel mould with high heat capacity to allow for a quick solidification. X-ray fluorescence spectroscopy (XRF analysis, Oxford Instruments, X-Strata 980) was performed to validate the intended composition of the alloys. To characterise the thermal properties such as melting point and thermal expansion of the respective alloys differential thermal analysis (DTA, Netzsch, Jupiter STA449C) and thermodilatometry (WSK, taBase 500) have been carried out under inert conditions (Ar 4.8). Thermal expansion of the ground and defatted materials was studied in the temperature range from -100 to $+850\,^{\circ}C$, applying a heating rate of $5\,^{\circ}C\,min^{-1}$.

2.2 Copper–iron alloy tapes In order to establish a biaxial texture the ground CuFe ingots were cold rolled into thin sheets ($\leq 150\,\mu m$, thickness reduction $\geq 90\%$) and subsequently heat treated in reducing argon–hydrogen atmosphere (6.5% H_2, v/v). The annealing conditions are given in Table 1.

Field emission scanning electron microscopy (SEM, Zeiss LEO 1540 XB) has been performed to investigate the influence of the annealing step on the microstructure of the surface (see Fig. 1).

To observe the texture present in the specimen XRD, psi scans, phi scans and pole figure measurements using a Philips Pro X'Pert diffractometer (CuK_α radiation) were done.

All samples necessary for tensile strength measurements were annealed at the same time to ensure an equal thermal history for all specimens. Tensile strength measurements were performed according to EN 10002-1 using the same setup (Messphysik BETA 200-4 with 5 kN load cell) as described by Staller et al. [10]. To avoid any influence of the specimen production on the texture and therefore on the ultimate tensile strength, the samples were brought into rectangular shape ($\sim 9 \times 100 \times 0.15\,mm^3$) prior to the annealing step. The strain was applied parallel to the rolling direction of the samples.

Magnetisation data of the annealed samples ($3 \times 9 \times 0.1\,mm^3$) at 5 K were obtained by using a SQUID magnetometer (Quantum Design, MPSM-2) Magnetisation loops were measured at 5 K in the range of $\pm 800\,kA\,m^{-1}$, applying the magnetic field parallel (along the longest sample axis) to the sample.

Table 1 Annealing conditions of the alloys.

alloy	T_{max} / °C	dwell time / min
CuFe0.37	750	30
CuFe0.91	850	30

Heating rate: $8\,^{\circ}C\,min^{-1}$.

Table 2 Thermal constants.

alloy	mp / °C	$\alpha_{-100/850\,^{\circ}C}$
Cu-ETP	1083	18.6×10^{-6}
CuFe0.37	1079	19.2×10^{-6}
CuFe0.91	1092	20.1×10^{-6}

3 Results and discussion

3.1 Bulk samples The thermal constants given in Table 2 (melting point mp, thermal expansion coefficient α) show that the values for the alloys are very similar to those found for pure copper. As pointed out in Fig. 2 the thermal expansion of all specimens is almost equal. Deviations can only be found at temperatures $>500\,^{\circ}C$ for pure copper. The maximum deviation of the thermal expansion coefficient is $\sim 10\%$.

3.2 Tape samples The microstructure of the metal tapes is significantly influenced by the annealing process. The micrographs in Fig. 1 compare the surface of cold rolled material before and after annealing. It is found that the surface of the rolled specimens has an imbricate structure caused by the elongation along the rolling direction. This mechanical treatment induces a movement along the gliding planes which produces a rod type structure. The single rods have typical diameters of 0.5–1.0 μm and a length of minimum 2 μm. The latter cannot be determined precisely from these measurements but is not expected to be much larger from simple geometrical and mechanical considerations. These rods are stapled over each other and the typical grain structure cannot be observed any longer, whereas the thermally treated samples exhibit a smoother surface and the typical grain structure.

Figure 3 shows the 2θ XRD of the two rolled and annealed alloys. The {200} orientation is predominant, but also some minor polycrystalline fraction is observed for CuFe0.91. Since the {200} K_β peak at $2\theta \sim 45^{\circ}$ showed no valid information, this region was left out. The peak at $2\theta \sim 54^{\circ}$ resulting from a not perfectly Ni filtered CuK_α radiation was left out as well.

The phi scans given in Fig. 4, display the good in-plane alignment of the alloys. Full width at half maximum (FWHM) for CuFe0.37 are 7.3 and 6.8° for CuFe0.91, respectively, approving these alloys to be promising candidates as substrates for superconductors. Out-of-plane texture is investigated using psi scans (Fig. 5), resulting in FWHM values of 7.2° for both alloys.

To reduce AC losses due to magnetic hysteresis effect it is of decisive importance to reduce this ferromagnetic feature as much as possible [11]. Figure 6 depicts the magnetisation data of the two alloys taken at 5 K. The data obtained for CuFe0.37 and CuFe0.91 prove the ferromagnetism of the compounds, yielding a saturation magnetisation of $M_s < 0.25$ and $< 0.35\,\mu Wb\,m\,kg^{-1}$, respectively. Table 3

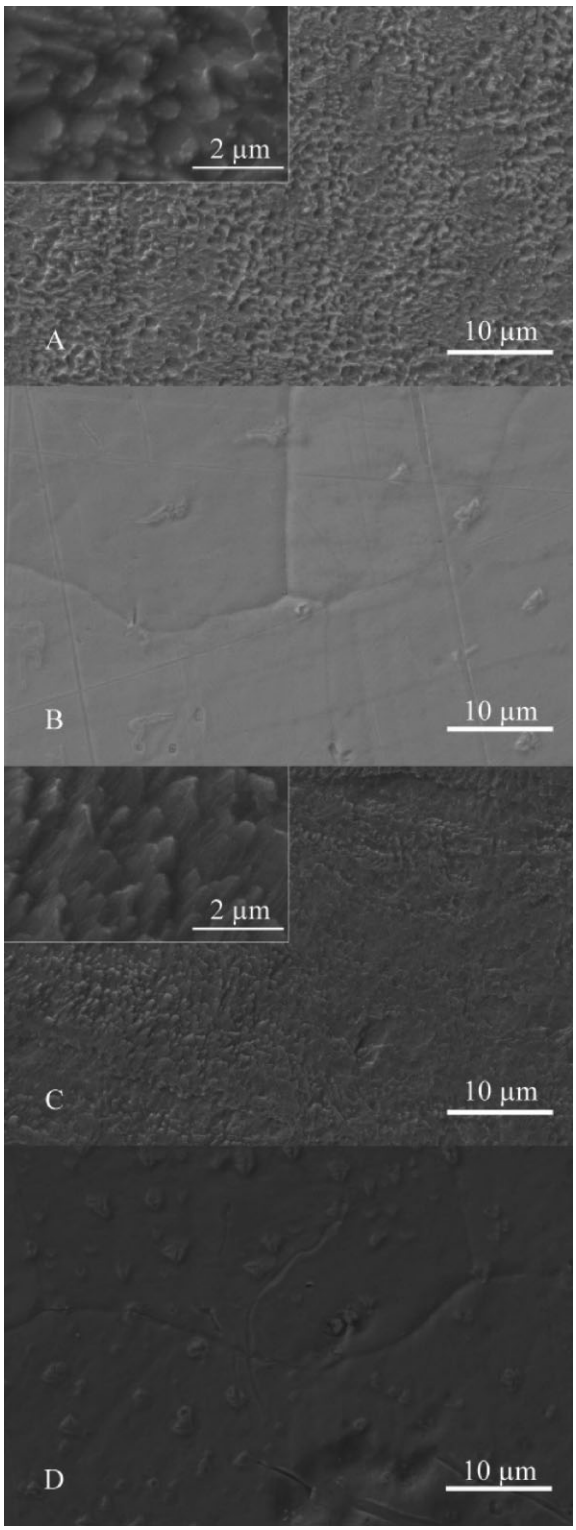

Figure 1 SEM micrographs of CuFe0.37 (A and B) and CuFe0.91 (C and D) showing the microstructure of the cold rolled (A and C) and heat treated (B and D) specimen.

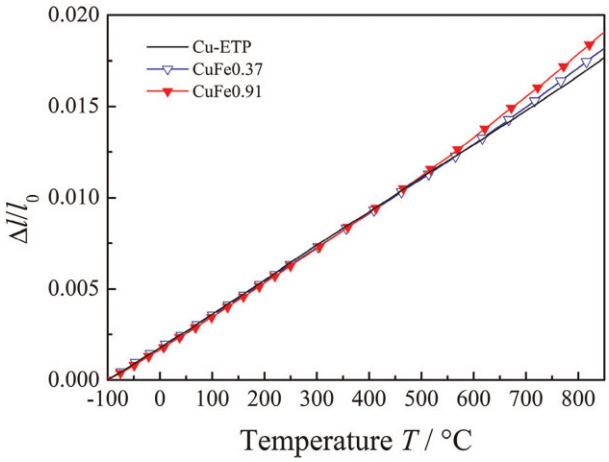

Figure 2 (online colour at: www.pss-a.com) Comparison of the thermal expansion.

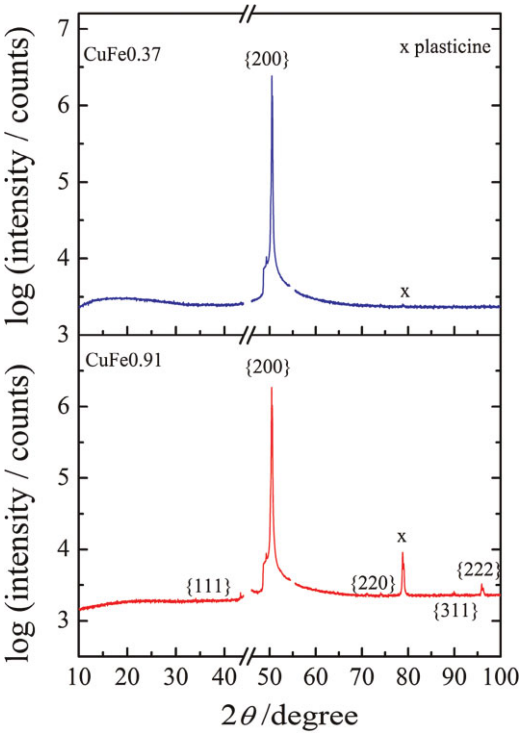

Figure 3 (online colour at: www.pss-a.com) 2θ XRD scans of CuFe0.37 (top) and CuFe0.91 (bottom). Since the {200} K_β peak at $2\theta \sim 45^\circ$ showed no important information, this region was cut out.

gives a comparison of the magnetisation data for different materials suitable as substrate for superconductors.

Figure 7 shows the yield strength curves for both materials before and after the annealing step. It can be seen that due to the thermal treatment which is necessary to achieve the biaxial texture, the average ultimate tensile strength drops from 468.7 to 214.0 MPa for CuFe0.37 and

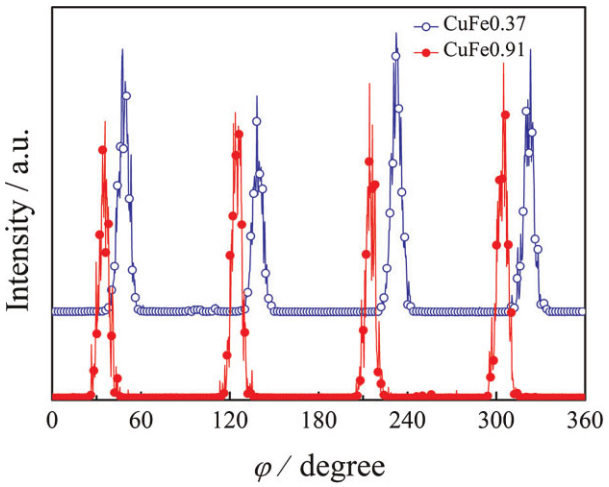

Figure 4 (online colour at: www.pss-a.com) Phi scans of CuFe0.37 and CuFe0.91, giving FWHM values of 7.3 and 6.8°, respectively.

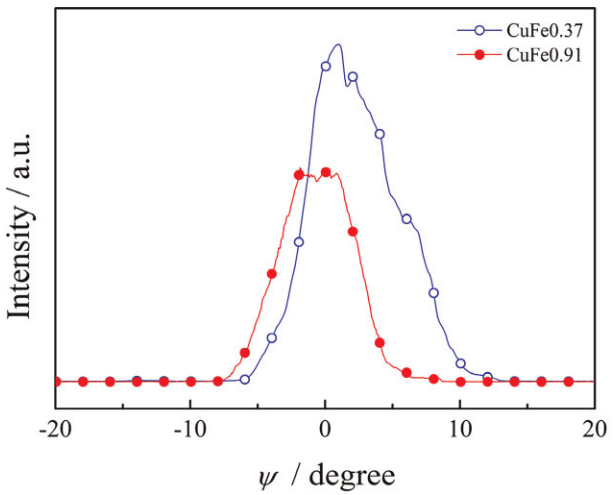

Figure 5 (online colour at: www.pss-a.com) Psi scans of CuFe0.37 and CuFe0.91. Similar FWHM values of 7.2° are retrieved for both alloys.

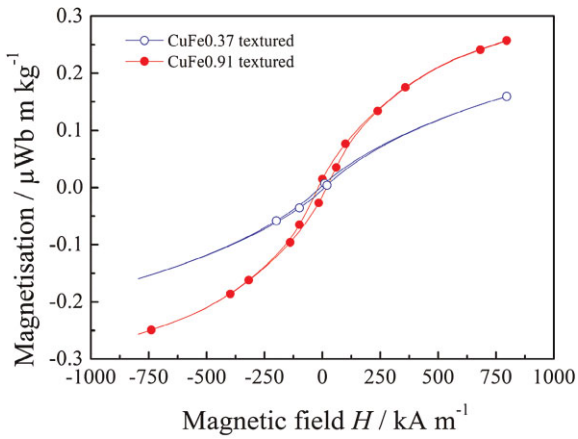

Figure 6 (online colour at: www.pss-a.com) Magnetisation loops of CuFe0.37 and CuFe0.91 at 5 K.

Table 3 Magnetisation data obtained for various metallic substrates obtained at 5 K.

material	M_s / μWb m kg^{-1}
Ni [a]	71.7
Ni–$W_{3at.\%}$ [a]	45.7–46.9
CuFe2.35 [a]	5.4
CuFe0.37	<0.25
CuFe0.91	<0.35

[a]Taken from Ref. [10].

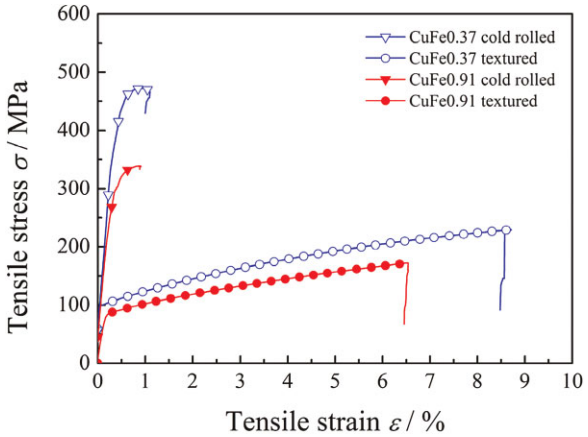

Figure 7 (online colour at: www.pss-a.com) Stress–strain curves for the rolled and textured Cu–Fe alloys.

from 381.8 to 161.3 MPa for CuFe0.91, respectively. Compared to pure copper and CuFe2.35 (Varanasi et al. [9]) the alloys, presented in this study, show a significantly improved tensile strength.

4 Conclusion Two Cu–Fe alloys with a sharp biaxial texture could be obtained using a thermal treatment step. Phi scans of CuFe0.37 and CuFe0.91 (FWHM 7.3, 6.8°) prove good in-plain alignment of the alloys, whereas (FWHM of 7.2°) for out-of-plane texture for both alloys was achieved. Magnetisation data collected from both samples display an anticipated saturation magnetisation <0.25 μWb m kg^{-1} for CuFe0.37 and <0.35 μWb m kg^{-1} for CuFe0.91, respectively.

Ultimate tensile strength depends on the initial cross section and the annealing step necessary to create the biaxial texture of the samples. The average tensile strength drops from 468.7 to 214.0 MPa for CuFe0.37 and from 381.8 to 161.3 MPa for CuFe0.91, respectively. Compared to the values given in the literature for pure Cu and CuFe2.35, these alloys have an enhanced ultimate tensile strength.

Acknowledgements We wish to thank the Austrian science fund (Fonds zur Förderung der wissenschaftlichen Forschung in Österreich) for the funding of the induction furnace within the

project 17420-N07. We also thank Margit Kriechbaum for assistance with the yield strength measurements.

References

[1] A. Goyal, D. P. Norton, J. D. Budai, M. Paranthaman, E. D. Specht, D. M. Kroeger, D. K. Christen, Q. He, B. Saffian, F. A. List, D. F. Lee, P. M. Martin, C. E. Klabunde, E. Hartfield, and V. K. Sikka, Appl. Phys. Lett. **69**, 1795 (1996).
[2] J. R. Thompson, A. Goyal, D. K. Christen, and D. M. Kroeger, Phys. C **307**, 169 (2002).
[3] J. Eickemeyer, R. Hühne, A. Güth, C. Rodig, H. Klauß, and B. Holzapfel, Supercond. Sci. Technol. **21**, 105012 (2008).
[4] K. T. Kim, J. H. Lim, J. H. Kim, J. Joo, W. Nah, B. K. Ji, B.-H. Jun, C.-J. Kim, and G.-W. Hong, Phys. C **412-414**, 859 (2004).
[5] A. Tuissi, E. Villa, M. Zamboni, J. E. Evetts, and R. I. Tomov, Phys. C **372-376**, 759 (2002).
[6] N. A. Rutter, A. Goyal, C. E. Valle, F. A. List, D. F. Lee, L. Heatherly, and D. M. Kroeger, Supercond. Sci. Technol. **17**, 527 (2008).
[7] C. Cantoni, D. K. Christen, E. D. Specht, M. Varela, J. R. Thompson, A. Goyal, C. Thieme, Y. Xu, and S. J. Pennycook, Supercond. Sci. Technol. **17**, 341 (2004).
[8] J. L. Soubeyroux, C. E. Bruzek, A. Girard, and J. L. Jorda, IEEE Trans. Appl. Supercond. **15**, 2687 (2005).
[9] C. V. Varanasi, P. N. Barnes, and N. A. Yust, Supercond. Sci. Technol. **19**, 85 (2006).
[10] O. Staller, C. Mitterbauer, and K. Mayr, Cent. Eur. J. Chem. **6**, 535 (2008).
[11] A. O. Ijaduola, J. R. Thompson, A. Goyal, C. L. H. Thieme, and K. Marken, Phys. C **403**, 163 (2004).